VIP Monolayers Very Important Paper

International Edition: DOI: 10.1002/anie.201508473
German Edition: DOI: 10.1002/ange.201508473

Synthesis of a Two-Dimensional Covalent Organic Monolayer through Dynamic Imine Chemistry at the Air/Water Interface

*Wenyang Dai[+], Feng Shao[+], Jacek Szczerbiński, Ryan McCaffrey, Renato Zenobi, Yinghua Jin, A. Dieter Schlüter, and Wei Zhang**

Abstract: *A two-dimensional covalent organic monolayer was synthesized from simple aromatic triamine and dialdehyde building blocks by dynamic imine chemistry at the air/water interface (Langmuir–Blodgett method). The obtained monolayer was characterized by optical microscopy, scanning electron microscopy, and atomic force microscopy, which unambiguously confirmed the formation of a large (millimeter range), unimolecularly thin aromatic polyimine sheet. The imine-linked chemical structure of the obtained monolayer was characterized by tip-enhanced Raman spectroscopy, and the peak assignment was supported by spectra simulated by density functional theory. Given the modular nature and broad substrate scope of imine formation, the work reported herein opens up many new possibilities for the synthesis of customizable 2D polymers and systematic studies of their structure–property relationships.*

In recent years, there has been growing interest in developing unimolecularly thin two-dimensional polymeric materials, which can be considered as structural analogues of graphene.[1–5] A 2D polymer (2DP) is a monomolecular covalent network of periodically linked monomers.[1] 2DPs are particularly interesting for surface and materials science, owing to their intriguing properties and potential applications (separation, coating, sensing), which are distinct from those of bulk polymeric materials. Current 2DP synthetic methods mainly rely on [4+4] cycloaddition reactions under UV irradiation, either in the solid state[6–8] or at an air/water interface.[9,10] Although a series of 2DPs have been successfully synthesized through such photochemical processes, the monomer structure has thus far been limited to anthracene-containing building blocks, and the resulting 2DPs are linked through C–C single bonds, which impedes their applications as electronic or optoelectronic materials. Moreover, the development of alternative synthetic approaches that are not based on photochemistry would facilitate large-scale production of 2DPs. To promote diversity in 2DP design and synthesis and to make use of the great potential of this intriguing class of materials, the development of alternative synthetic approaches for 2DPs is highly desired.

Dynamic covalent chemistry (DCC)[11–13] has emerged as a powerful synthetic approach for well-defined molecular architectures. It has been successfully utilized in the synthesis of shape-persistent macrocycles, molecular cages, and polymer frameworks.[14–16] Dynamic imine chemistry, which deals with Schiff base formation, has been widely applied in small-molecule and polymer synthesis.[17–19] We envisioned that imine chemistry would be a promising approach for the preparation of 2DPs owing to the dynamic nature of imine bond formation, which enables self-correction mechanisms and allows the molecular structure to be formed under thermodynamic control. Although Schiff base reactions have been used to prepare ordered covalent organic frameworks (COFs)[20–23] with thicknesses far from the sub-nanometer level and extended monolayer structures by on-surface approaches,[24–26] to the best of our knowledge, applications of such reactions to covalent monolayer synthesis under ambient conditions at an air/water interface have never been reported. This work presents the first example of such a monolayer synthesis; the use of a Langmuir trough and horizontal Schäfer-type transfer resulted in a 0.7 nm thin freestanding monolayer sheet, whose lateral dimension are in the range of tens of micrometers. The structure of this aromatic polyimine monolayer was investigated by atomic force microscopy (AFM) for thickness determination, scanning electron microscopy (SEM), optical microscopy, and tip-enhanced Raman spectroscopy (TERS), where the signal assignment was based on density functional theory (DFT) simulations.

The imine-linked 2D covalent monolayer was synthesized from two simple aromatic building blocks: terephthalaldehyde (**1**) and 1,3,5-trihexyl-2,4,6-tris(4-aminophenyl)benzene (**2**; Scheme 1). Compound **2** bears three *n*-hexyl groups. At the air/water interface, these three hydrophobic groups likely stand up on the surface and point into the air while all of the phenyl rings stay in the interface, anchored by the three hydrophilic amino groups. Such a conformation would render compound **2** a good candidate for the interfacial synthesis of a polyimine monolayer. Ideally, the triamine and dialdehyde building blocks orient themselves so that strain-free imine linkages will be formed. If there are undesired bond formations leading to strained or disordered subunits in the

[*] R. McCaffrey, Dr. Y. Jin, Prof. Dr. W. Zhang
Department of Chemistry and Biochemistry
University of Colorado
Boulder, CO 80309 (USA)
E-mail: wei.zhang@colorado.edu
W. Dai,[+] Prof. Dr. A. D. Schlüter
Department of Materials, Institute of Polymers
Swiss Federal Institute of Technology, ETH Zürich
8093 Zürich (Switzerland)
F. Shao,[+] J. Szczerbiński, Prof. Dr. R. Zenobi
Department of Chemistry and Applied Biosciences
Swiss Federal Institute of Technology, ETH Zürich
8093 Zürich (Switzerland)
[+] These authors contributed equally to this work.

Supporting information for this article is available on the WWW under http://dx.doi.org/10.1002/anie.201508473.

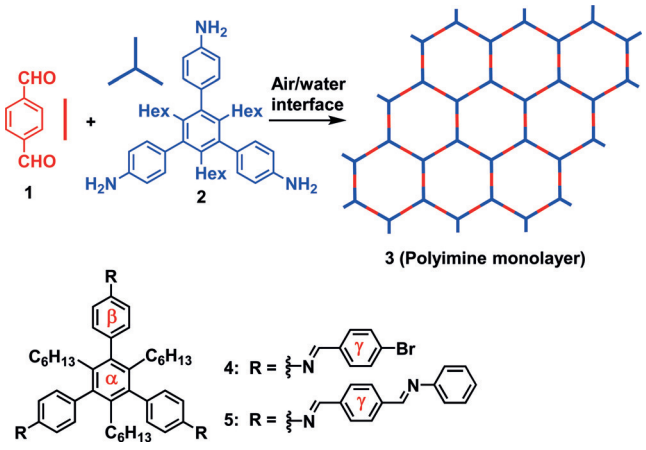

Scheme 1. Synthesis of a polyimine network from dialdehyde **1** and triamine **2** and chemical structures of the model compounds **4** and **5**. The presented network omits possible defects.

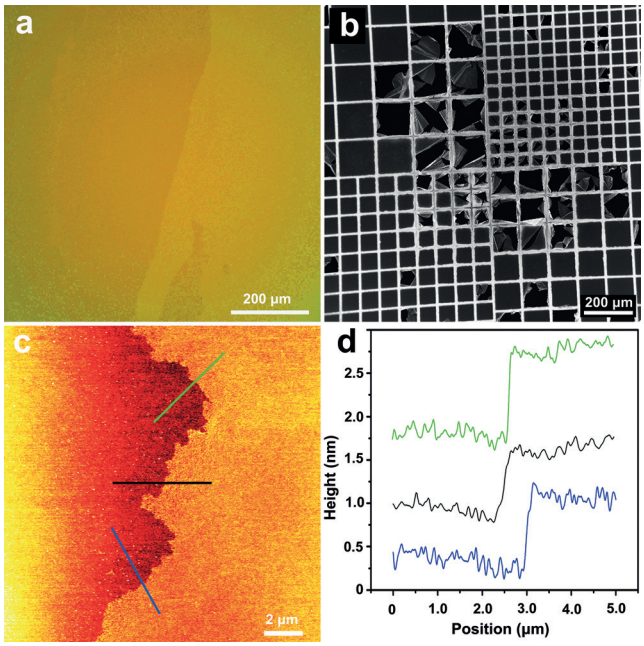

Figure 1. Microscopy images of polyimine sheet **3**. a) Optical microscopy image of the film; yellow areas (right) show the underlying SiO_2/Si substrate, and the orange areas (left) show the sheet. b) SEM images of polyimine sheets on TEM grids. c) Tapping-mode AFM height image of a polyimine monolayer after vertical transfer onto a 285 nm thick SiO_2 on Si substrate. d) Corresponding line profiles. The lines in (c) indicate where the height profile was recorded.

resulting network, the reversibility of the imine bond formation could enable self-correction processes, thus leading to the thermodynamically favored polymer product with an ordered structure.

A dilute solution of monomers **1** and **2** (3:2 molar ratio, 1 mg mL^{-1}) in chloroform was spread at an air/water interface, and the surface pressure (SP) versus the mean molecular area (MMA) isotherm was recorded. The isotherm reproducibly shows a phase transition at low surface pressures before a steep increase in pressure is observed (Figure S1). The MMA of the mixture of monomers **1** and **2** was determined to be about 120 Å^2 at a pressure of 3 mN m^{-1}. The interface was monitored by Brewster angle microscopy (BAM; Figure S2). The monomers exhibited very good spreadability in the early stage of compression (for an SP just above zero), and quite homogenous polymer sheets were observed without the formation of typical islands (Figure S2). After further compression, the polymer sheets with strip/ribbon shapes began to coalesce and at SP = 3 mN m^{-1}, a coherent, smooth polymer layer was formed, indicating that the monomers were spread with a homogeneous thickness over the entire interface. This isotherm study led us to perform all interfacial polymerizations at SP = 3 mN m^{-1}, with a catalytic amount of trifluoroacetic acid added to catalyze the imine formation. For structure elucidation, imine model compound **4**, which closely resembles the repeating units of the monolayer, was also prepared from triamine **2** and 4-bromobenzaldehyde (1:3 molar ratio). For the same reason, the solution-phase polymerization of amine **2** and aldehyde **1** was conducted to obtain a 3D polymer network (**6**) with the same chemical connectivity as monolayer **3**, but with uncontrolled thickness and random orientation.

The interfacial polymerization was run overnight. The resulting polymer sheet (**3**) was transferred onto silicon wafers and TEM grids, and characterized by optical microscopy, SEM, and AFM (Figure 1). Figure 1a shows that the films can be transferred to solid substrates with sizes in the range of several hundreds of micrometers. A SEM image of the homogenous film on a TEM grid illustrates that even holes with sizes of 100 × 100 μm^2 were fully spanned. Ruptures of the films were a frequent encounter, which was attributed to the mechanical strain caused during transfer and/or drying. Assuming that the films on the grids are monolayers, they are comparably stable under electron-beam irradiation and do not burn immediately when the beam is focused. This may be helpful when structure elucidation is to be conducted by high-resolution TEM under cryogenic conditions. To confirm that the polyimine film was a monolayer, a height analysis by tapping-mode AFM was conducted, which revealed a thickness of about 0.7 nm and the smooth surface of the polymer sheet (Figure 1c,d).

To gain first insights into the chemical structure of the obtained polyimine sheet (**3**), the monolayer was characterized by tip-enhanced Raman spectroscopy (TERS), and the peak assignment was supported by DFT simulations (Figure 2 and Figure 3). TERS combines the advantages of scanning probe microscopy (SPM) and Raman spectroscopy, and enables the simultaneous recording of the topography and chemical fingerprint of samples with nanoscale resolution.[27] TERS has been shown to have a sensitivity down to the single-molecule level,[28,29] which is vital for obtaining insightful Raman spectra of a single 2D sheet.[30] The average TER spectrum of a polyimine monolayer (**3**) was obtained from the mean of the TER spectra of 20 spots randomly chosen from different sheet samples (Figure 3 and S5). The confocal Raman spectra of both monomers (**1** and **2**), imine model compound **4** (Figure S4), and 3D polyimine network **6**, which was obtained by solution-phase polymerization, were also

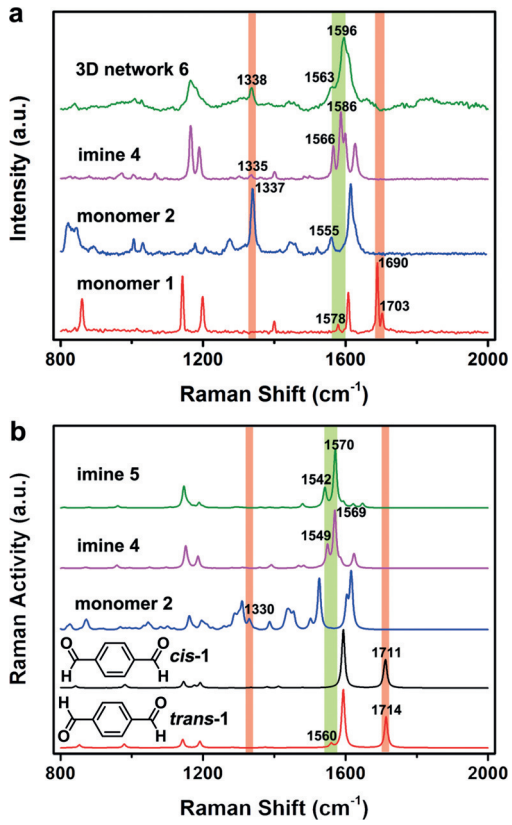

Figure 2. a, b) The normalized confocal Raman spectra (a) and the Raman spectra simulated by DFT calculations (b) of corresponding compounds are in good agreement with each other. The bands discussed in the text are highlighted.

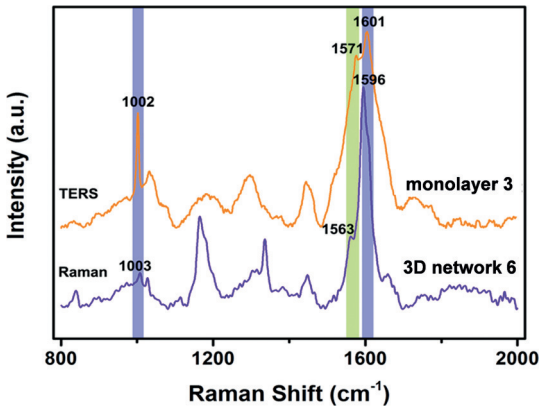

Figure 3. Normalized average tip-enhanced Raman spectrum of monolayer polyimine **3** deposited on a gold substrate and confocal Raman spectrum of 3D polyimine network **6**. The bands discussed in the text are highlighted.

investigated. DFT calculations at the BP86/RI/TZVP level of theory were carried out for the monomers and model systems to study the expected differences in their Raman spectra.[31,32] Both conformations of aldehyde **1**, which arise from the different orientation of the carbonyl group (*cis* or *trans* with respect to each other), were considered in the calculations. Triimine **5** was used as a finite-sized polymer unit structure for the simulations (Figure S4).

First, we studied the confocal Raman spectra of the monomers (**1** and **2**), model compound **4**, and 3D polyimine network **6** by measuring variations in the intensity of the bands corresponding to vibrations of the CHO, NH_2, and C=N groups (Figure 2). In the spectrum of monomer **1**, the bands at 1690 and 1703 cm^{-1} correspond to the aldehyde C=O stretching vibrations (1711 and 1714 cm^{-1} in the simulated spectra, see Movie S1). Such bands are absent in the spectra of the imine model compound (**4**) and 3D polyimine network **6**, as well as in the TER spectrum of monolayer polyimine **3** (Figure 3). The band at 1337 cm^{-1} (1330 cm^{-1} in the simulated spectrum) in the spectrum of amine **2** corresponds to a stretching vibration of the β-ring and wagging of its NH_2 group (Movie S1). Correspondingly, the intensity of this band is significantly reduced in the confocal Raman spectrum of imine model compound **4** (ca. 1335 cm^{-1}) and 3D polyimine network **6** (ca. 1338 cm^{-1}; Figure 2a). The simulated and confocal Raman spectra consistently demonstrate that the CHO and NH_2 groups are present only in trace amounts after the polymerization, both for imine model compound **4** and 3D polyimine network **6**. Therefore, we not only have unequivocal evidence for the existence of the proposed imine bonds in the sheets, but we also know that, at least within the method's sensitivity, there are no defects in terms of end groups.

The DFT calculations (Figure 2b) indicate that the peaks around 1550 cm^{-1} for the polymer model compound (**5**; 1542 and 1570 cm^{-1}) and the imine model compound (**4**; 1549 and 1569 cm^{-1}) correspond to stretching vibrations of the newly formed C=N bonds located between the β- and γ-rings, accompanied by stretching of those two rings (Movie S1). Consistently, these bands are absent in the simulated spectra of both monomers **1** and **2** (Figure 2b). The very weak band at 1560 cm^{-1} in the spectrum of monomer **1** (*trans*) likely results from a benzene ring stretching vibration (Movie S1).

The above predictions of the DFT calculations fully support the experimental data obtained for the imine model compound (**4**) and the polyimines (**3** and **6**). The ring and C=N stretching vibrations are clearly visible in the confocal Raman spectrum of imine model compound **4** (1566 and 1586 cm^{-1}). They are also present in the spectrum of the 3D polyimine network **6** (Figure 2a). However the bands at 1563 and 1596 cm^{-1} are substantially broadened, most likely owing to intermolecular interactions within the polymer network. The average TER spectrum of a monolayer of polyimine **3** clearly shows the presence of the C=N stretching vibration band at 1571 cm^{-1} and 1601 cm^{-1}. Remarkably, these bands are even more pronounced in the TER spectrum of a monolayer of polyimine **3** than in the confocal Raman spectrum of 3D polyimine network **6**. The peak for the β-ring breathing mode at 1002 cm^{-1} was also more intense and explicit in the TER spectrum of monolayer polyimine **3** than in the confocal Raman spectrum of the 3D polyimine network **6**. The increased intensity and slight shifts of the bands in the TER spectrum of monolayer polyimine **3** likely arise from the change of molecular geometry on the surface (surface selection rule, Figure S6).[33,34] Overall, the collected Raman and TER spectra confirm the formation of a conjugated

system (β-N=C-γ) upon polymerization, which is fully supported by the results of the DFT calculations.

In conclusion, we have successfully synthesized an imine-linked covalent organic monolayer through dynamic imine chemistry at the air/water interface. The monolayer was characterized by optical microscopy, SEM, AFM, and TERS. The formation of such smooth, coherent, large, and free-standing polyimine monolayers is unprecedented, and represents a significant step towards the preparation of conjugated two-dimensional polymers for electronic or optoelectronic applications. Although we cannot yet disclose the molecular structure of the sheets by using imaging techniques such as STM, we found that the AFM-determined sheet thickness, showing the monolayer nature, in combination with Raman-based evidence for both the existence of imine bonds and the absence of end groups (within the limits of resolution), provides strong arguments for the proposed structure. Currently, these imine-linked polymer sheets are explored by further characterization studies along with the substrate scope of this synthetic approach. Our findings will be reported in due course.

Experimental Section

Polyimine monolayers were prepared on a Langmuir–Blodgett trough (KSV 2000 System 2, KSV NIMA, Finland) using Millipore water, and placed on an antivibration table in a dust-reduced environment. The surface pressure was measured with a Wilhelmy balance with a precision of 0.01 $mN\,m^{-1}$. A typical experiment was performed as follows: 25 μL of a 1.0 $mg\,mL^{-1}$ solution of monomer **1** was pre-mixed with 75 μL of a 1.0 $mg\,mL^{-1}$ solution of monomer **2** in $CHCl_3$. The resulting solution (50 μL) was spread on a water surface with a microliter syringe. The solvent was allowed to evaporate for 30 min, then the compression was carried out at a rate of 3 $mm\,min^{-1}$ until the surface pressure stabilized at 3 $mN\,m^{-1}$. Trifluoroacetic acid (0.35 mL) was then added dropwise into the solution without disturbing the self-assembled monomer layer. After 12 h of polymerization at 3 $mN\,m^{-1}$, the pre-submerged substrate (e.g., a silicon wafer) was pulled up at a constant rate of 0.5 $mm\,min^{-1}$. After drying at room temperature, the collected monolayer was subjected to optical microscopy, SEM, and AFM.

DFT calculations were carried out with Turbomole 6.4 software. All calculations were performed by applying the BP86 functional, taking advantage of the RI approximation. The TZVP set of basis functions was chosen. The optimized geometry and the calculated vibrational modes were visualized using TmoleX software.

Confocal Raman and TERS measurements were performed on a combined STM/Raman microscope (Ntegra Spectra, NT-MDT, Zelenograd, Russia) following routine procedures as described previously.[30] Briefly, all confocal Raman spectra were obtained by averaging 10 accumulations with an acquisition time of 10 s each, using a 632.8 nm HeNe laser at an incident power of 1.7 mW for excitation. The 3-fold deposition of the 2D polymer monolayer sheet on a template-stripped gold substrate was described in more detail in our previous work.[30] An exposure time of 3 s and 30 accumulations with 0.3 mW laser power (632.8 nm) were used for the TERS measurements of the 2D polymer monolayer sheet. All measurements were performed several times at numerous locations on the sample for the sake of reproducibility. All experimental Raman spectra were normalized, baseline-corrected (Polynom mode with degree 8), and smoothed (Savitsky–Golay mode with degree 4) by the commercial software Labspec 5 (HORIBA, Germany).

Acknowledgements

W.Z. thanks the Alfred P. Sloan Foundation and the ETH Zürich for financial support. W.D. thanks the Swiss National Science Foundation for financial support. F.S. thanks the Chinese Scholarship Council for a Ph.D. student fellowship. We thank the High Performance Computing Team at ETH Zurich for help with the DFT calculations and Dr. Lothar Opilik for helpful discussions.

Keywords: dynamic covalent chemistry · imines · monolayers · polymers · Raman spectroscopy

How to cite: *Angew. Chem. Int. Ed.* **2016**, *55*, 213–217
Angew. Chem. **2016**, *128*, 221–225

[1] J. Sakamoto, J. van Heijst, O. Lukin, A. D. Schlüter, *Angew. Chem. Int. Ed.* **2009**, *48*, 1030–1069; *Angew. Chem.* **2009**, *121*, 1048–1089.
[2] J. W. Colson, W. R. Dichtel, *Nat. Chem.* **2013**, *5*, 453–465.
[3] Z. H. Xiang, D. P. Cao, L. M. Dai, *Polym. Chem.* **2015**, *6*, 1896–1911.
[4] Y. Zang, T. Aoki, M. Teraguchi, T. Kaneko, L. Q. Ma, H. G. Jia, *Polym. Rev.* **2015**, *55*, 57–89.
[5] M. Lackinger, *Polym. Int.* **2015**, *64*, 1073–1078.
[6] P. Kissel, R. Erni, W. B. Schweizer, M. D. Rossell, B. T. King, T. Bauer, S. Gotzinger, A. D. Schlüter, J. Sakamoto, *Nat. Chem.* **2012**, *4*, 287–291.
[7] M. J. Kory, M. Worle, T. Weber, P. Payamyar, S. W. van de Poll, J. Dshemuchadse, N. Trapp, A. D. Schlüter, *Nat. Chem.* **2014**, *6*, 779–784.
[8] P. Kissel, D. J. Murray, W. J. Wulftange, V. J. Catalano, B. T. King, *Nat. Chem.* **2014**, *6*, 774–778.
[9] P. Payamyar et al., *Adv. Mater.* **2014**, *26*, 2052–2058.
[10] D. J. Murray, D. D. Patterson, P. Payamyar, R. Bhola, W. T. Song, M. Lackinger, A. D. Schlüter, B. T. King, *J. Am. Chem. Soc.* **2015**, *137*, 3450–3453.
[11] S. J. Rowan, S. J. Cantrill, G. R. L. Cousins, J. K. M. Sanders, J. F. Stoddart, *Angew. Chem. Int. Ed.* **2002**, *41*, 898–952; *Angew. Chem.* **2002**, *114*, 938–993.
[12] P. T. Corbett, J. Leclaire, L. Vial, K. R. West, J. L. Wietor, J. K. M. Sanders, S. Otto, *Chem. Rev.* **2006**, *106*, 3652–3711.
[13] Y. Jin, C. Yu, R. J. Denman, W. Zhang, *Chem. Soc. Rev.* **2013**, *42*, 6634–6654.
[14] Y. H. Jin, Q. Wang, P. Taynton, W. Zhang, *Acc. Chem. Res.* **2014**, *47*, 1575–1586.
[15] A. Wilson, G. Gasparini, S. Matile, *Chem. Soc. Rev.* **2014**, *43*, 1948–1962.
[16] Q. Ji, R. C. Lirag, O. S. Miljanic, *Chem. Soc. Rev.* **2014**, *43*, 1873–1884.
[17] M. E. Belowich, J. F. Stoddart, *Chem. Soc. Rev.* **2012**, *41*, 2003–2024.
[18] C. D. Meyer, C. S. Joiner, J. F. Stoddart, *Chem. Soc. Rev.* **2007**, *36*, 1705–1723.
[19] N. M. Rue, J. L. Sun, R. Warmuth, *Isr. J. Chem.* **2011**, *51*, 743–768.
[20] F. J. Uribe-Romo, J. R. Hunt, H. Furukawa, C. Klock, M. O'Keeffe, O. M. Yaghi, *J. Am. Chem. Soc.* **2009**, *131*, 4570–4571.
[21] S. Y. Ding, J. Gao, Q. Wang, Y. Zhang, W. G. Song, C. Y. Su, W. Wang, *J. Am. Chem. Soc.* **2011**, *133*, 19816–19822.
[22] X.-H. Liu, C.-Z. Guan, S.-Y. Ding, W. Wang, H.-J. Yan, D. Wang, L.-J. Wan, *J. Am. Chem. Soc.* **2013**, *135*, 10470–10474.
[23] Y. Jin, Y. Zhu, W. Zhang, *CrystEngComm* **2013**, *15*, 1484–1499.
[24] X. H. Liu, C. Z. Guan, D. Wang, L. J. Wan, *Adv. Mater.* **2014**, *26*, 6912–6920.

[25] R. Tanoue, R. Higuchi, N. Enoki, Y. Miyasato, S. Uemura, N. Kimizuka, A. Z. Stieg, J. K. Gimzewski, M. Kunitake, *ACS Nano* **2011**, *5*, 3923 – 3929.
[26] X. H. Liu, Y. P. Mo, J. Y. Yue, Q. N. Zheng, H. J. Yan, D. Wang, L. J. Wan, *Small* **2014**, *10*, 4934 – 4939.
[27] T. Schmid, L. Opilik, C. Blum, R. Zenobi, *Angew. Chem. Int. Ed.* **2013**, *52*, 5940 – 5954; *Angew. Chem.* **2013**, *125*, 6054 – 6070.
[28] W. H. Zhang, T. Schmid, B. S. Yeo, R. Zenobi, *Isr. J. Chem.* **2007**, *47*, 177 – 184.
[29] W. H. Zhang, B. S. Yeo, T. Schmid, R. Zenobi, *J. Phys. Chem. C* **2007**, *111*, 1733 – 1738.
[30] L. Opilik, P. Payamyar, J. Szczerbiński, A. P. Schutz, M. Servalli, T. Hungerland, A. D. Schlüter, R. Zenobi, *ACS Nano* **2015**, *9*, 4252 – 4259.
[31] J. Neugebauer, M. Reiher, B. A. Hess, *J. Chem. Phys.* **2002**, *117*, 8623 – 8633.
[32] L. Yu, C. Greco, M. Bruschi, U. Ryde, L. De Gioia, M. Reiheet, *Inorg. Chem.* **2011**, *50*, 3888 – 3900.
[33] S. Jiang, Y. Zhang, R. Zhang, C. Hu, M. Liao, Y. Luo, J. Yang, Z. Dong, J. G. Hou, *Nat. Nanotechnol.* **2015**, *10*, 865 – 869.
[34] M. Moskovits, J. S. Suh, *J. Phys. Chem.* **1984**, *88*, 5526 – 5530.

Received: September 9, 2015
Published online: November 19, 2015

